Journal Pre-proofs

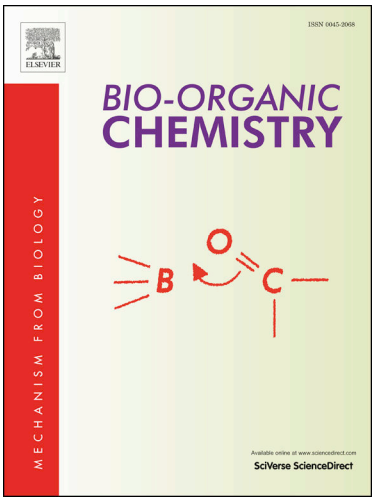

Synthesis and antitumor activity of α,β-unsaturated carbonyl moiety- containing oleanolic acid derivatives targeting PI3K/AKT/mTOR signaling pathway

Shi-Sheng Wang, Qiao-Li Zhang, Peng Chu, Ling-Qi Kong, Guang-Zhe Li, Yue-Qing Li, Li Yang, Wei-Jie Zhao, Xiu-Han Guo, Ze-Yao Tang

PII: S0045-2068(20)31333-X
DOI: https://doi.org/10.1016/j.bioorg.2020.104036
Reference: YBIOO 104036

To appear in: *Bioorganic Chemistry*

Received Date: 19 January 2020
Revised Date: 24 April 2020
Accepted Date: 19 June 2020

Please cite this article as: S-S. Wang, Q-L. Zhang, P. Chu, L-Q. Kong, G-Z. Li, Y-Q. Li, L. Yang, W-J. Zhao, X-H. Guo, Z-Y. Tang, Synthesis and antitumor activity of α,β-unsaturated carbonyl moiety- containing oleanolic acid derivatives targeting PI3K/AKT/mTOR signaling pathway, *Bioorganic Chemistry* (2020), doi: https://doi.org/10.1016/j.bioorg.2020.104036

This is a PDF file of an article that has undergone enhancements after acceptance, such as the addition of a cover page and metadata, and formatting for readability, but it is not yet the definitive version of record. This version will undergo additional copyediting, typesetting and review before it is published in its final form, but we are providing this version to give early visibility of the article. Please note that, during the production process, errors may be discovered which could affect the content, and all legal disclaimers that apply to the journal pertain.

© 2020 Elsevier Inc. All rights reserved.

Journal Pre-proofs

Title: Synthesis and antitumor activity of α,β-unsaturated carbonyl moiety-containing oleanolic acid derivatives targeting PI3K/AKT/mTOR signaling pathway

Graphic Abstract

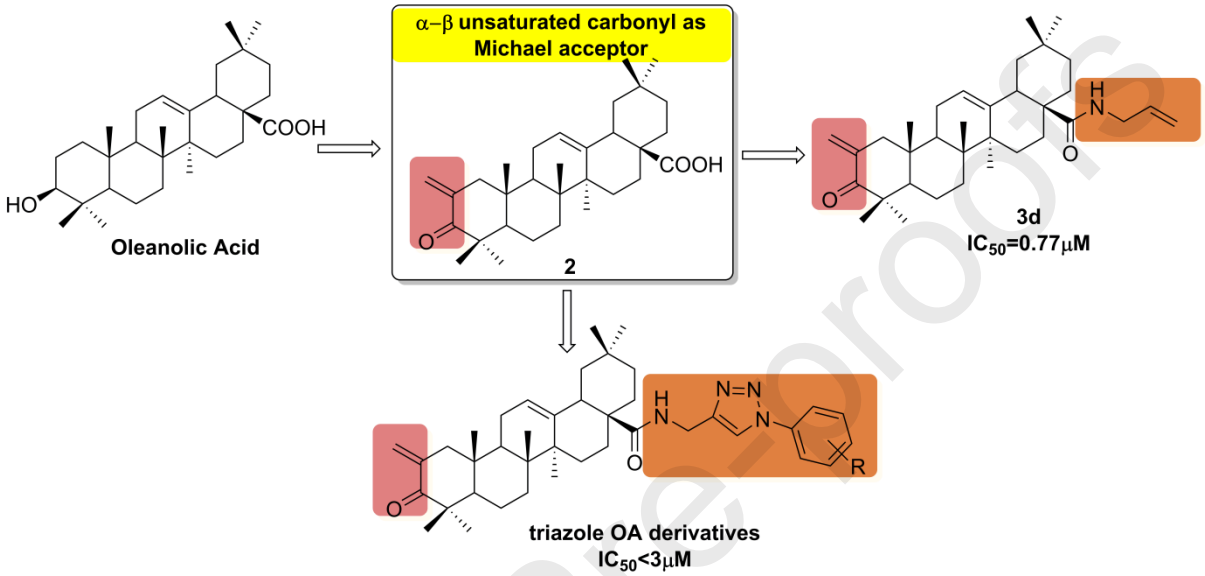

Highlights

- 21 new oleanolic acid derivatives containing α,β-unsaturated carbonyl were synthesized.
- Most synthesized compounds exhibited potent antiproliferative activities against MCF-7, HepG2 and HeLa cells.
- Compound 3d displayed the most potent inhibitory activity in MCF-7 cells with an IC_{50} of 0.77 μM.
- Compound 3d inhibited the cells migration, arrested cell cycle at S phase and targeted PI3K/AKT/mTOR signaling pathway in MCF-7 cells.

Journal Pre-proofs

Synthesis and antitumor activity of α,β-unsaturated carbonyl moiety-containing oleanolic acid derivatives targeting PI3K/AKT/mTOR signaling pathway

Shi-Sheng Wang[1], Qiao-Li Zhang[1], Peng Chu[2], Ling-Qi Kong[1], Guang-Zhe Li[1], Yue-Qing Li[1], Li Yang[1], Wei-Jie Zhao[1], Xiu-Han Guo[1*], Ze-Yao Tang[2*]

1. Department of Pharmacy, School of Chemical Engineering, Dalian University of Technology, Dalian 116024, China
2. Department of Pharmacology, Dalian Medical University, Dalian 116044, China

*Corresponding author: kakumicin@dlut.edu.cn (Xiu-Han Guo); tangzeyao@163.com (Ze-Yao Tang).

Abstract

Oleanolic acid (OA) and its semi-synthetic derivatives have been reported to have a wide range of biological activities. The introduction of electrophilic Michael acceptor group can increase the reactivity of OA to cellular targets and thus improve the anti-tumor activity. In this work, a series of novel α,β-unsaturated carbonyl derivatives of OA were designed and synthesized. Their *in vitro* cytotoxic activity against MCF-7, HepG2 and HeLa cells were tested. Most derivatives exhibited improved cell growth inhibitory activity, especially for **3d** with an IC_{50} of 0.77 μM in MCF-7 cells. Moreover, **3d** inhibited the migration of MCF-7 and HeLa cells at the concentration of 4 μM. Flow cytometric analysis revealed that **3d** induced cell apoptosis and S phase arrest in a concentration-dependent manner. Western blotting experiment demonstrated that **3d** inhibited the phosphorylation of AKT and mTOR. These results suggest that this series of OA derivatives bearing exocyclic methylene ketone pharmacophore are promising anticancer agents as potential PI3K/AKT/mTOR pathway inhibitors.

Keywords: Oleanolic acid derivatives, anticancer, PI3K/AKT/mTOR signaling pathway, cell apoptosis induction, S phase arrest

1. Introduction

Pentacyclic triterpenoids are widely distributed in the plant kingdom. Oleanolic acid (OA, Fig.1) is one of the most well-known pentacyclic triterpenes[1,2], which has a wide range of biological activities including anti-inflammatory, hepatoprotective, antitumor, antiviral, antidiabetic, antimicrobial, antiparasitic and analgesic effects[3–5]. In the past decades, a large number of OA derivatives have been synthesized and explored for their antitumor[6], anti-angiogenic[7], anti-diabetic[8], antiviral[9], anti-inflammatory[10] and other activities. The antitumor and anti-inflammatory effects of OA have received the most attention and many semi-synthetic OA derivatives were reported to have improved activity. In the previous investigation of OA derivatives as anticancer agents in our laboratory, a series of Mannich base derivatives (SZC014, SZC015, SZC017, Fig.1) were synthesized and exhibited significant antitumor activities through various mechanisms, including inducing apoptosis in cancer cells, inhibiting AKT or NF-κB signaling pathway, promoting ROS production in a variety of cancer cell lines[11–17].

According to literatures on the modification of OA, the introduction of electrophilic Michael acceptor in rings A and C can increase the reactivity of OA to cellular targets, and thus improves the antitumor activity[18]. Some Michael acceptor derivatives of OA have entered clinical trials for cancer , such as 2-cyano-3,12-dioxooleana-1,9(11)-dien-28-oic acid (CDDO) and it methyl ester CDDO-Me[19,20] (Fig. 1), which possess an α-cyano-substituted α,β-unsaturated ketone (CUK) in ring A and an α,β-unsaturated ketone in ring C, respectively, and display potent anti-cancer, anti-inflammatory and anti-diabetic nephropathy (DN) activities. The CUK moiety in ring A can react with thiol(s) in Keap1 and IKKβ through Michael addition[21,22].

During the past decade, covalent targeting has been more and more widely used in the fields of drug design and molecular biology, especially in oncology[23,24]. Targeted covalent inhibitors are typically designed from reversible ligands by introducing an electrophilic covalent reactive group, such as α,β-unsaturated ketones/aldehydes/esters/amides, that reacts with a variety of thiols in cellular proteins via Michael addition[25–27]. However, the selectivity and safety remain challenging in the design of targeted covalent inhibitors. For example, in a phase III clinical trial, CDDO-Me caused heart failure in patients with stage 4

DN, which resulted in the termination of the clinical trial[28]. The highly reactive CUK moiety in CDDO-Me was considered to be responsible for the cytotoxic effects through depletion of mitochondrial glutathione[29]. Therefore, the proper reactivity and selectivity of an electrophilic covalent reactive group is crucial for designing an effective and safety covalent drug.

The compounds containing α,β-unsaturated carbonyl groups are widely distributed in biologically active molecules that have been used successfully in cancer therapeutics due to the ability to react with cellular thiols. In this study, with exocyclic methylene ketone as a Michael acceptor moiety, a series of novel α,β-unsaturated carbonyl-containing OA analogues were designed and synthesized. Their *in vitro* anticancer activities were investigated by MTT assay and flow cytometry analysis, and the effect on the PI3K/AKT/mTOR signaling pathway was validated with western blotting analysis.

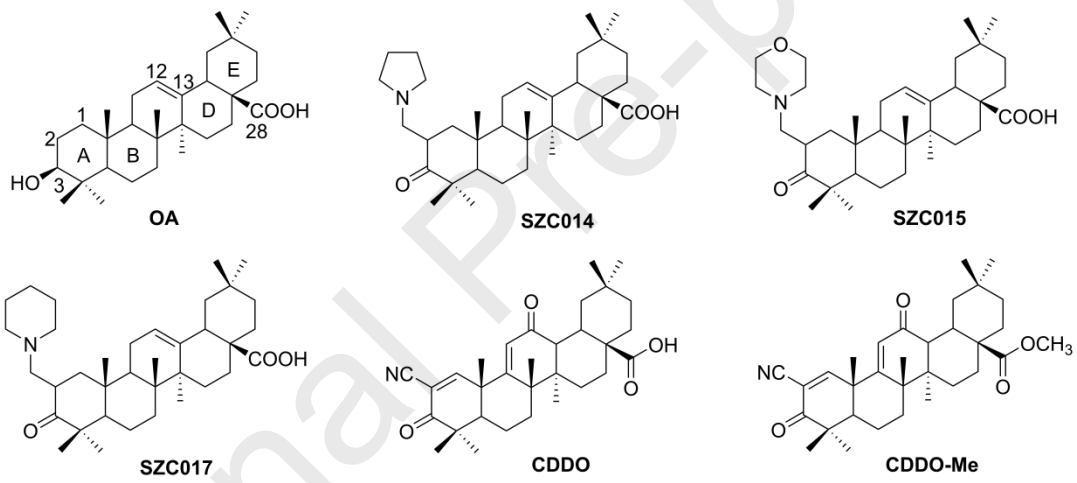

Fig.1. The chemical structures of oleanolic acid and its derivatives.

2. Results and discussion

2.1. Chemistry

The conjugated α,β-unsaturated carbonyl moiety is considered to be one of the most important functional groups as Michael acceptors in covalent drug discovery[25]. In order to improve the binding of OA derivatives with macromolecular targets, we here introduced exocyclic methylene ketone at 2, 3-position of the A ring as the Michael acceptor, followed by amidation of 28-COOH. As described in scheme 1, 3-oxo oleanolic acid **(1)** was first synthesized from OA by the oxidization of 3-OH to a carbonyl group with Jone's regent.

Journal Pre-proofs

Compound **1** was then converted to 2-methylene 3-oxo oleanolic acid **(2)** via Mannich reaction with paraformal dehyde and dimethylamine hydrochloride and subsequent Huffman elimination under alkaline condition. Finally, compound **2** underwent chlorination of 28-COOH and amidation with different amines to yield seven new derivatives **3a-3g** with different sizes of side chains.

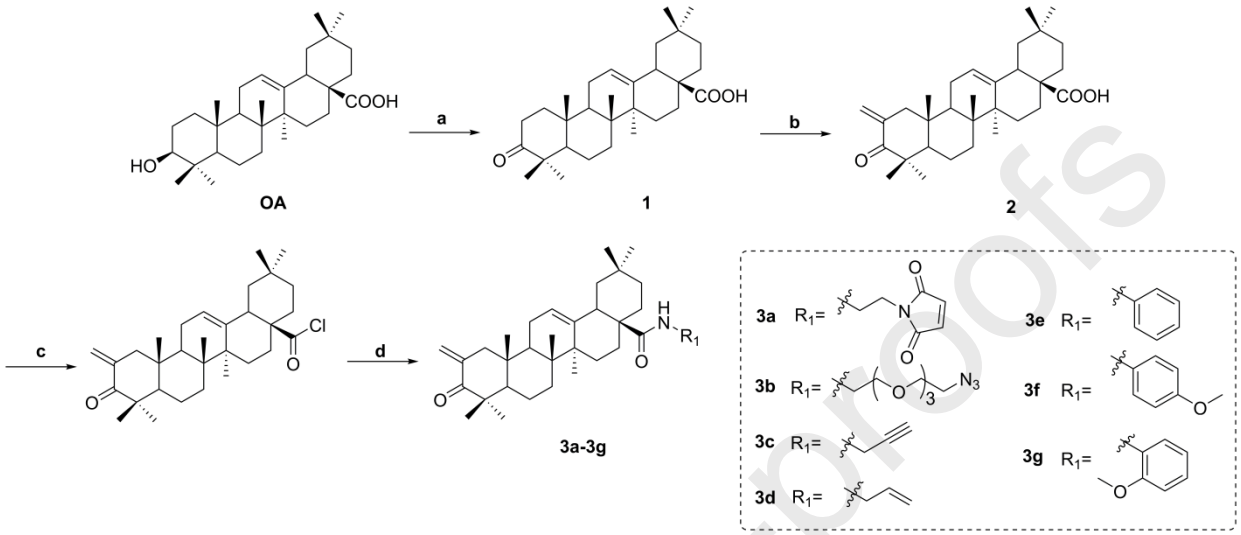

Scheme 1. Synthetic route to compounds **3a-3g**. Reagents and conditions: (a) Jone's reagent, acetone/ CH_2Cl_2(1:1), 0℃,90%. (b) i. paraformaldehyde, dimethylamine hydrochloride, DMF,100℃; ii.$NaHCO_3$(aq), 100℃,1h, 61%. (c) oxalyl chloride, DMF/ CH_2Cl_2,rt. (d) amine compounds,DIEA,CH_2Cl_2,rt,26%-90%.

1,2,3-triazole is a kind of essential nitrogen heterocyclic moiety which is widely applied in the construction of drug molecules, especially in the field of anticancer drugs[30] 1,2,3-triazole derivatives have attracted much attention in the field of medicinal chemistry due to their broad range of pharmacological properties and facile synthesis via click chemistry[31]. For further optimizing the substituents at C-28, we synthesized a series of novel OA derivatives **(4a-4n)** containing α,β-unsaturated carbonyls at ring A and benzene-substituted 1,2,3-triazole moieties at C-28. By a Cu-catalyzed click reaction, compounds **4a~4n** were synthesized with compound **3c** and aromatic azides (**5a-5n**), which were prepared from their corresponding anilines by diazotization with sodium nitrite under acidic conditions followed by displacement with sodium azide (Scheme.2).

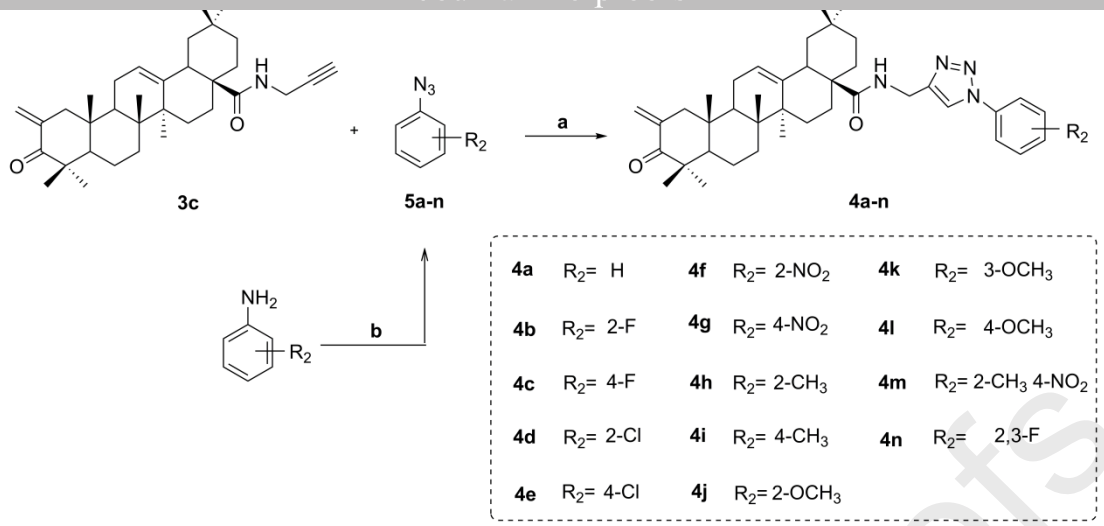

Scheme 2. Synthetic route to compounds **4a-4n**. Reagents and conditions: (a) sodium ascorbate, $CuSO_4$, BuOH/H_2O(1:1),room temperature(rt),overnight,41%-77%. (b) i. H_2O/HCl(1:1),$NaNO_2$(aq),0℃,2h; ii.NaN_3(aq), 0℃,1h.

2.2. Biology

2.2.1. Cytotoxicity assay

To evaluate the antitumor activity of the synthesized OA derivatives, we tested their inhibitory effects on the cell proliferation of MCF-7, HepG2 and HeLa cells by MTT assay using CDDO-Me as a positive control. As shown in table 1, compounds **3c**-**3f** displayed more potent inhibitory activity than the precursor compound **2**. Among them, compounds **3c** and **3d** with the smaller size of substituent at C-28 showed stronger inhibitory activity against MCF-7 proliferation with IC_{50} of 1.04 and 0.77 μM, respectively. Compared with **3e**, compound **3f** increased the cytotoxic effects whereas **3g** significantly decreased the cytotoxic effects, suggesting the position of methoxyl group at benzene ring is important for anti-proliferative effects of OA derivatives. Moreover, compound **3a** with a maleimide moiety at C-28 as a Michael acceptor showed weakest anti-proliferative effects. A long chain substituent at C-28 as in compound **3b** is also unfavorable to anti-proliferative effects.

Another series of OA derivatives **4a**-**4n**, which contain substituted phenyl 1,2,3-triazole moiety, showed almost equivalently high antiproliferative activity against three cancer cell lines. Compared respectively with **3e**-**3g**, compounds **4a**, **4l** and **4j** showed better inhibitory activity, indicating that the insertion of 1,2,3-triazole increased their anticancer activities. However, the substituents on the benzene ring, regardless of electron-withdrawing groups (-F,

-Cl, -NO_2) or electron-donating groups (-CH_3, -OCH_3), displayed little effects on their antitumor activity. Among these triazole -containing OA derivatives, **4a** and **4f** exhibited very strong anti-proliferative effects against HeLa cells with IC_{50} values of 1.14 and 1.12 μM, respectively, while **4k** exhibited most potent anti-proliferative effects against HepG2 cells with IC_{50} of 0.94 μM. As expected, all these compounds **2**, **3a-3g** and **4a-4n** showed much lower cytotoxicity than the positive control CDDO-Me, which might be attributed to the relatively weak eletrophilicity of α,β-unsaturated ketone compared with CUK moiety of CDDO-Me.

Table.1. *In vitro* anti-proliferative effects of OA derivatives against MCF-7, HepG2 and HeLa cells

Entry	Compds	IC_{50} (μM)[a]		
		MCF-7	HepG2	HeLa
1	2	7.13±0.63	12.83±3.15	6.16±0.48
2	3a	14.01±0.67	37.63±3.28	>50
3	3b	4.66±0.10	12.66±1.88	16.23±0.98
4	3c	1.04±0.07	3.13±0.88	2.08±0.56
5	3d	0.77±0.03	4.57±1.33	1.23±0.03
6	3e	2.81±0.13	6.98±0.30	2.00±0.16
7	3f	1.46±0.05	3.47±0.36	2.67±0.23
8	3g	7.44±0.38	7.73±0.11	11.60±0.10
9	4a	1.94±0.15	2.38±0.08	1.14±0.31
10	4b	2.86±0.25	1.42±0.08	1.36±0.34
11	4c	2.58±0.27	1.73±0.06	2.78±0.03
12	4d	2.22±0.13	2.42±0.12	1.32±0.24
13	4e	3.36±0.14	3.61±0.09	2.29±0.23
14	4f	1.40±0.17	3.90±0.31	1.12±0.12
15	4g	2.45±0.13	3.42±0.13	1.25±0.13
16	4h	2.09±0.13	1.92±0.10	2.32±0.29
17	4i	2.00±0.15	1.62±0.02	1.71±0.21
18	4j	1.69±0.04	1.41±0.06	2.19±0.10
19	4k	1.52±0.04	0.94±0.01	1.82±0.08
20	4l	1.29±0.04	1.38±0.05	1.60±0.10
21	4m	2.95±0.11	6.54±0.22	2.67±0.41
22	4n	1.93±0.05	1.97±0.16	1.84±0.09
23	CDDO-Me	0.67±0.02	0.26±0.02	-

[a]IC_{50}: The concentration that causes 50% inhibition of cell proliferation. Data are expressed as the means±SD from triplicate determination from three independent experiments.

*2.2.2 . Compound **3d** inhibited cell migration of MCF-7 and HeLa cells*

To investigate the effects of these OA derivatives on migration inhibition in tumor cells,

Journal Pre-proofs

Journal Pre-proofs

we used the *in vitro* scratch assay to measure the effect of compound **3d** on the migration ability of MCF-7 and HeLa cells. As shown in Fig.2, the migration rates of both MCF-7 and HeLa cells after 24 h from the scratch in **3d** (4μM) group were much smaller than those in the control group. These results indicated that **3d** significantly inhibited the migration of MCF-7 and HeLa cells in addition to their cell proliferation.

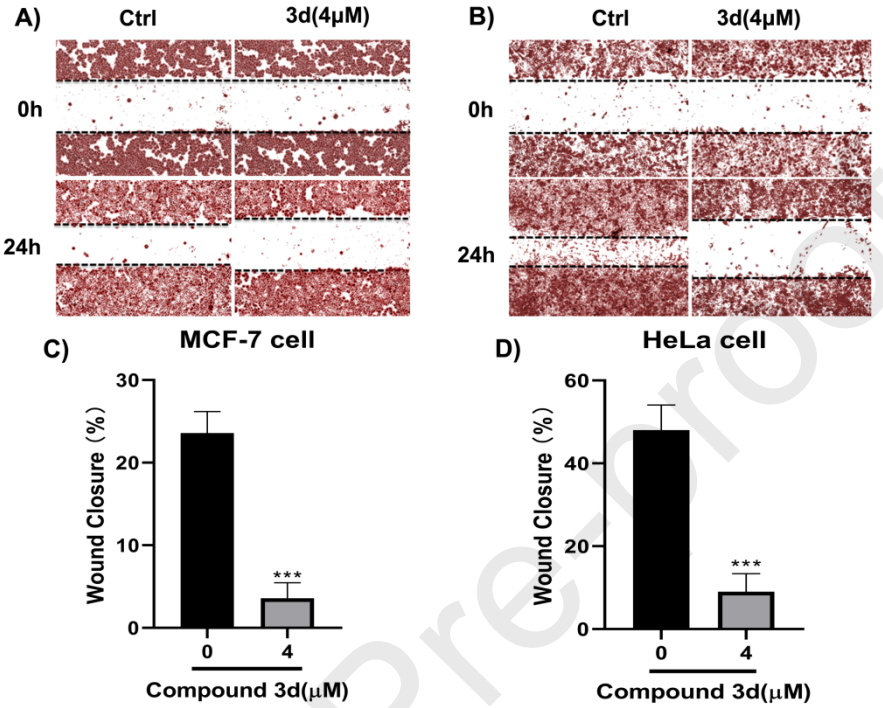

Fig.2. Compound **3d** inhibited migration of MCF-7 and HeLa cells. MCF-7 cells and HeLa cells were scratched by pipette and treated with **3d (4μM)**. After 24 h from the scratch, the migrated cells were photographed.(A) Compound **3d** inhibited MCF-7 cells migration.(B) Compound **3d** inhibited HeLa cells migration. (C) and (D) illustrate the percentage of wound closure in untreated control cells and 3d treated cells at 24h. Values are given as the means ± SD of each group of cells from three individual experiments. ***P < 0.001

*2.2.3. Compound **3d** induced apoptosis of MCF-7 cells*

The apoptosis of MCF-7 cells treated with various concentrations of **3d** for 24 h was examined. The cells were harvested and stained with Annexin V-FITC and propidium iodide (PI), and the percentages of apoptotic cells were determined by flow cytometry analysis. It was observed that treatment with **3d** induced apoptosis of MCF-7 cells in a dose-dependent manner. When treated with 2, 4 and 8 μM of **3d** for 24 h, the percentages of apoptotic cells were 5.44%, 19.02% and 57.59% (Q2 + Q3), respectively (Fig.3), while the vehicle control group treated with DMSO contained 2.71% apoptotic cells. This result demonstrated that the anti-proliferative activity observed in **3d**-treated MCF-7 cells involved with the cell apoptosis

induction.

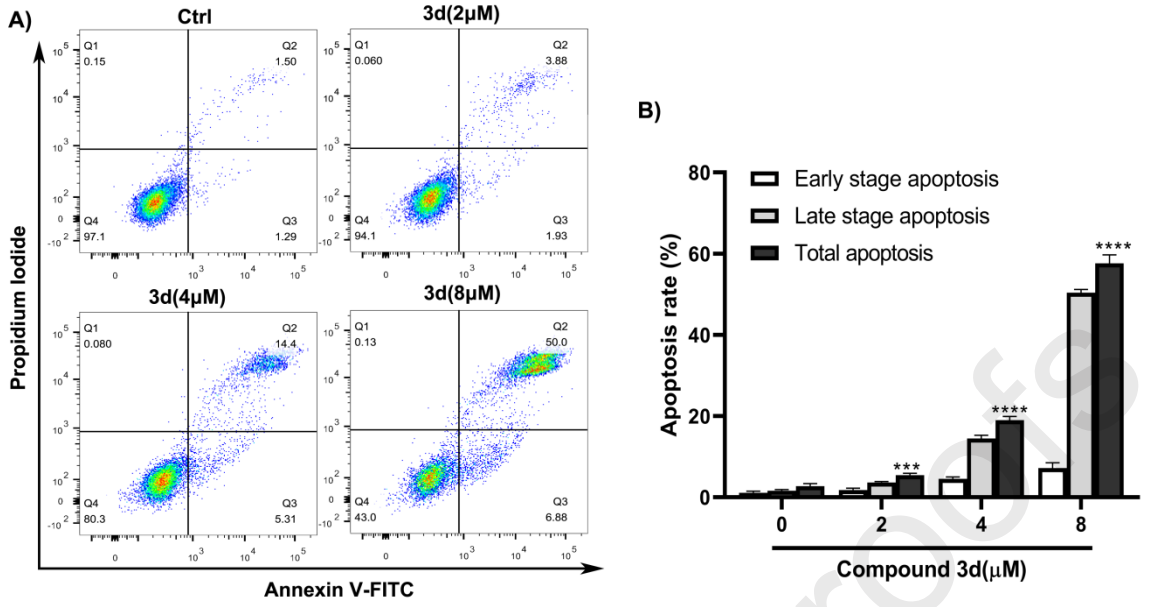

Fig.3. Flow cytometric evaluation of apoptosis based on Annexin V/PI double labeling. (A) Apoptosis of MCF-7 cells treated with **3d** (2,4,8 μM) for 24 h before harvested and analyzed by flow cytometry.(B) Apoptosis rate is displayed through the histogram. It was observed that treatment with **3d** induced apoptosis in MCF-7 cells in a dose-dependent manner. Results are representative images or expressed as the means ± SD of three individual experiments. ***P < 0.001, ****P < 0.0001.

*2.2.4. Target Prediction of compound **3d** in its anticancer action*

Although the anticancer effects of OA and its derivatives have been extensively investigated by many researchers, the definite targets and underlying mechanisms remain ambiguous until now. In this study, we used Pharma DB database in Discovery Studio software to predict the target of compound **3d** (FitValue≥0.9), and as a result, a total of 103 proteins were obtained. Then all proteins were input into DAVID 6.8, a bioinformatics analysis tool, to predict the KEGG (Kyoto Encyclopedia of Genes and Genomes) pathway [32]. The results were displayed in a bubble chart (Fig.4), and it was found that these enriched proteins affect cells through multiple pathways, including PI3K/AKT, TNF pathway and cell cycle.

Journal Pre-proofs

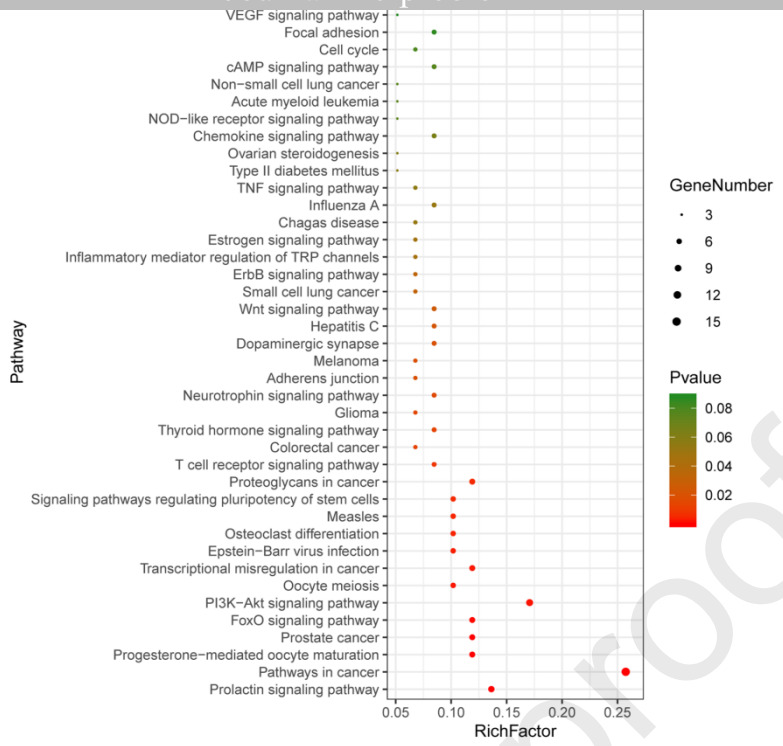

Fig.4. KEGG pathway of all predicted target proteins for compound **3d**. The top 40 most significant canonical signaling pathways are displayed.

The protein-protein interaction (PPI) of the predicted proteins was then analyzed using the STRING database [33] and 15 most important protein interactions were identified (Fig.5). The further KEGG pathway analysis of these 15 proteins suggested that these pathways were related to the cell cycle and cell apoptosis (Table 2).

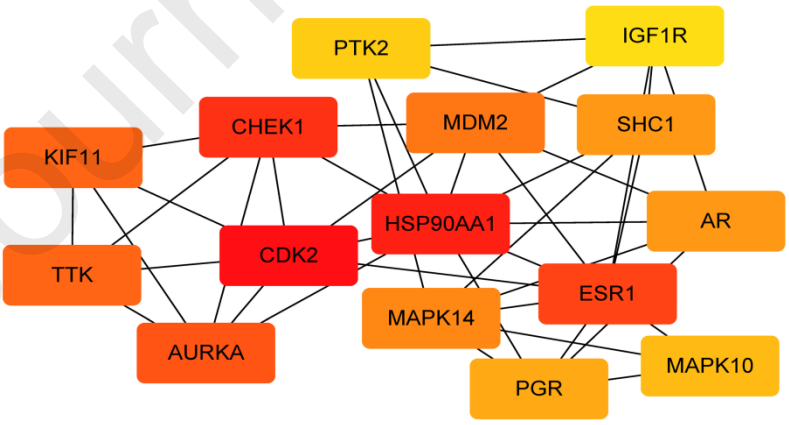

Fig.5. Protein interaction network construction and analysis using the cytohubba plug-in in cytoscape 3.6.0 statistical software, to determine the most important 15 protein interactions.

Table.2.KEGG pathway analysis of key proteins

Term	Count	PValue	Genes
Cell cycle	4	3.00E-04	TTK, MDM2, CHEK1, CDK2
p53 signaling pathway	3	2.52E-03	MDM2, CHEK1, CDK2
Oocyte meiosis	3	4.21E-03	AR, AURKA, CDK2
Proteoglycans in cancer	3	6.78E-03	MAPK14, ESR1, MDM2
PI3K-AKT signaling pathway	3	2.10E-02	HSP90AA1, MDM2, CDK2

*2.2.5. Compound **3d** induced S phase arrest in MCF-7 cells*

Cell cycle arrest is often observed during programmed cell death. Enlightened by the KEGG pathway analysis of key proteins, the effect of **3d** on the cell cycle of MCF-7 cells was determined by flow cytometric experiments. Upon treatment with **3d** at 2, 4 and 8 μM for 24 h, the percentage of cells at the different phases of cell circle was determined as shown in Fig.6. A dose-dependent accumulation of cells was observed at the S phase, increasing from 40.0% in the untreated cells to 50.8% in the cells treated with 8 μM **3d**. It is worth noting that the low concentration group at 2 μM of **3d** exhibited an unremarkable increase in the S phase cell proportion (43.0%), suggesting that some other mechanisms might be involved in inhibiting cell growth beside the S phase arrest.

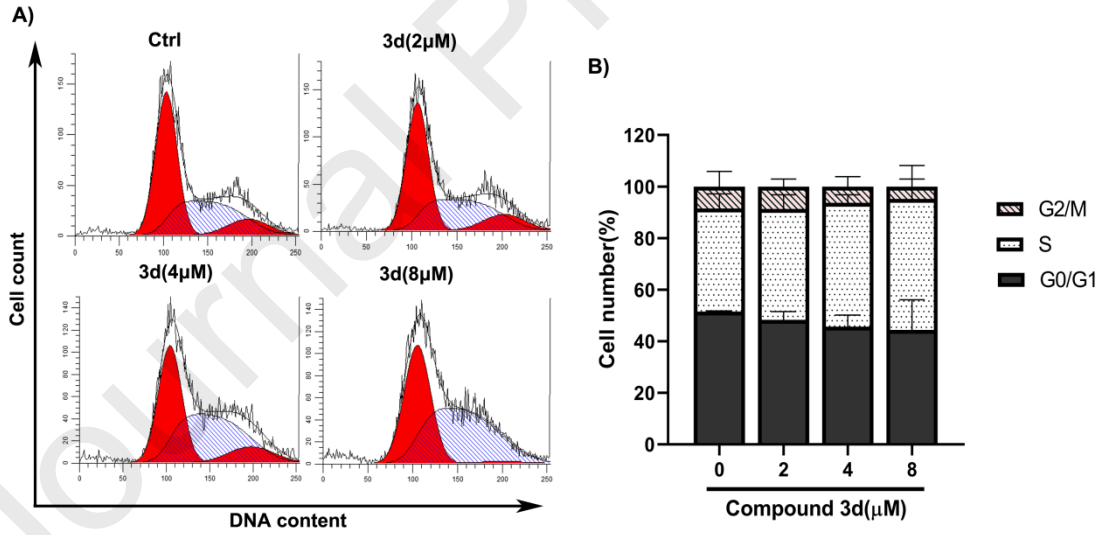

Fig.6. Compound **3d** induced S phase arrest in MCF-7 cells. MCF-7 cells were treated with **3d** at 2, 4, 8μM concentration for 24 h prior to analysis. The cell cycle was evaluated by propidium iodide staining. For the analysis, only live cells were selected. Untreated cells were taken as a control. (A) Effects of compound **3d** on the cell-cycle distribution in MCF-7 cells. (B) Bar graph proportions of cells in G1, S and G2/M phases. Results are representative images or expressed as the mean ± SD of three individual experiments.

Journal Pre-proofs

2.2.6. Inhibitory effect of 3d on the PI3K/AKT/mTOR Signaling Pathways

PI3K/AKT/mTOR signaling pathway plays an important role in occurrence and progression of tumor and drug resistance by inducing survival, differentiation and vascularization, and thus becomes an attractive target for cancer treatment [34–36]. Previous studies demonstrated that OA derivative **SZC015** displayed anti-cancer activity by inhibiting the PI3K/AKT/mTOR signaling pathway in human MCF-7 cells and other cancer cell lines[37]. The KEGG pathway analysis suggested that **3d** might exert its anticancer activity via PI3K/AKT/mTOR pathway. The effects of **3d** on the PI3K/AKT/mTOR signaling pathway were explored by western blotting. As shown in Fig.7, treatment with **3d** downregulated the levels of phosphorylation-AKT (p-AKT) and phosphorylation-mTOR (p-mTOR) in MCF-7 cells, which are known mediators of cell proliferation and inhibition of apoptosis. Moreover, the p-AKT/AKT ratio and p-mTOR level were significantly decreased in **3d** treatment groups in a concentration-dependent (Fig.7C and 7D) and time-dependent manner (Fig. 7E and 7F).

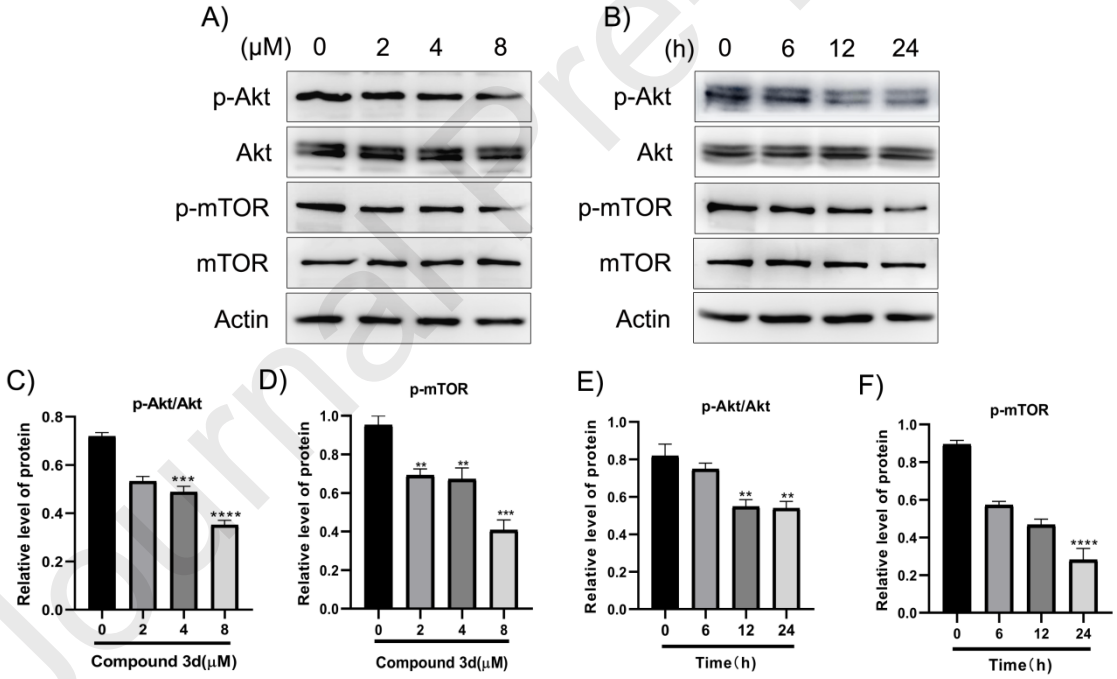

Fig.7. Effect of **3d** on PI3K/AKT/mTOR signaling pathway by western blot assay. (A) the changes of proteins expression in MCF-7 cells treated with **3d** (2, 4, and 8μM) for 12 h. (B) the changes of proteins expression in MCF-7 cells treated with **3d** (4μM) for 0,6,12 and 24 h. The statistical analysis of p-AKT/AKT ratio (C, E) and the expression of p-mTOR (D, F) in MCF-7 cells. Results are representative images or expressed as the mean ± SD of three individual experiments. **P < 0.01, ***P < 0.001.

3. Conclusion

In summary, we designed and synthesized a series of **OA** derivatives containing α,β-unsaturated carbonyl moiety and various amide substituents, and evaluated their anticancer activity against MCF-7, HepG2 and HeLa cell lines. Most derivatives showed much more potent anti-proliferative activity than OA, especially for **3d** against MCF-7 cells (IC_{50}=0.77 μM) and **4k** against HepG2 cells (IC_{50}=0.94 μM). Moreover, **3d** can significantly arrest the cell cycle of MCF-7 cells in the S phase and induce apoptosis of MCF-7 cells with 57.59% of total apoptosis rate. Besides inhibiting cell proliferation, **3d** can significantly inhibit the migration of MCF-7 and HeLa cells at concentration of 4 μM. In the preliminary study of anticancer mechanism of **3d**, the target prediction by KEGG analysis supplied multiple signaling pathways including PI3K/AKT pathway. Western blotting analysis validated that **3d** blocks phosphorylation of AKT and mTOR in MCF-7 cells, thus inactivates the PI3K/AKT/mTOR pathway, suggesting **3d** might be a potential PI3K/AKT/mTOR pathway inhibitor with the ability to induce apoptosis and suppress cell migration. Other related pathways and protein targets are presumably involved in the anticancer effect of this series of **OA** derivatives and will be further investigated in the future.

4. Experimental

4.1 Chemical synthesis

In the synthesis of derivatives of OA, all commercially available reagents, solvents and chemicals were used without further purification. The synthetic reactions were carried out at ambient temperature and the products were purified by column chromatography (silica gel; petroleum ether/ethyl acetate) to afford pure compounds. ^{1}H and ^{13}C NMR spectra were recorded on a Bruker Avance Ⅱ 400 MHz spectrometer, using TMS as an internal standard. Chemical shifts are given as δ values in parts per million (ppm) and coupling constants (J) are given in hertz (Hz). HRMS data were obtained on a LTQ Orbitrap XL instrument operating in multimode. Thin-layer chromatographic (TLC) separations were carried out on precoated silica gel plates. The purity of final compounds was determined to be >95% by HPLC analysis.

4.1.1. 3-Oxo-olean-12-en-28-oic acid（1）

10.0 g (21.9 mmol) of OA was added to 500 mL dichloromethane: acetone (v:v 1:1) and

Journal Pre-proofs
dissolved by stirring at 0 °C, and then Jones reagent was added dropwise to the mixture. The reaction mixture was continuously stirred at 0 °C for 30 minutes. The reaction solution was concentrated and 300 mL cooling $NaHCO_3$ and 300 mL EtOAc were added to produce a precipitation which was filtrated and dried. The crude products were recrystallized using methanol at 0 °C to yield a white solid (9.0 g, yield 90%). ^{1}H NMR (400 MHz, $CDCl_3$) δ 5.30 (t, *J* = 3.4 Hz, 1H), 2.84 (dd, *J* = 13.8, 4.2 Hz, 1H), 2.55(m, 1H), 2.36 (m,1H), 1.15 (s, 3H), 1.08 (s, 3H), 1.05 (s, 3H), 1.03 (s, 3H), 0.93 (s, 3H), 0.91 (s, 3H), 0.81 (s, 3H) ppm. ^{13}C NMR (101 MHz, $CDCl_3$) δ 217.72, 184.03, 143.64, 122.40, 55.30, 47.43, 46.89, 46.58, 45.81, 41.02, 39.27, 39.10, 36.80, 34.14, 33.80, 33.05, 32.40, 32.15, 30.68, 27.67, 26.44, 25.84, 23.56, 23.48, 22.89, 21.44, 19.54, 17.00, 15.01, 14.12 ppm .

4.1.2. 2-methylene-3-Oxo-olean-12-en-28-oic acid（2）

Compound **1** 2.5 g (5.5 mmol) was dissolved in 100 mL anhydrous DMF, to which dimethylamine hydrochloride 624 mg (7.7 mmol), paraformaldehyde 231 mg and acetic acid (0.3 mL) were added. The reaction mixture was stirred at 100℃ for 1.5 h. The mixture was cooled, adjusted to pH 8 with saturated aqueous $NaHCO_3$, and stirred at 100 ℃ for 1 h. The reaction solutionwas cooled, poured into brine and extracted with EtOAc. The organic phase was washed with saturated aqueous $NaHCO_3$ and brine and dried over anhydrous Na_2SO_4. After filtration and evaporation under reduced pressure, the yielded crude product was then purified with silica column chromatography (petroleum ether: ethyl acetate=5:1) to obtain compound **2** (1.6 g, yield 61%) as a white solid. HPLC: Purity 99.8%. mp: 228-232℃. ^{1}H NMR (400 MHz, $CDCl_3$) δ 5.99 (t, *J* = 2.1 Hz, 1H), 5.32 (t, *J* = 3.4 Hz, 1H), 5.16 (s, 1H), 2.85 (dd, *J* = 13.6, 4.1 Hz, 1H), 2.64 (d, *J* = 15.2 Hz, 1H), 2.13 (d, *J* = 15.1 Hz, 1H), 1.16 (s, 3H), 1.13 (s, 3H), 1.04 (s, 3H), 0.94 (s, 3H), 0.93 (s, 3H), 0.91 (s, 3H), 0.81 (s, 3H) ppm. ^{13}C NMR (101 MHz, $CDCl_3$) δ 207.52, 184.68, 143.77, 142.09, 123.94, 122.52, 54.27, 46.89, 45.96, 45.56, 41.96, 41.19, 39.32, 36.99, 34.84, 33.97, 33.23, 32.54, 32.14, 28.38, 27.83, 27.08, 25.92, 25.45, 23.71, 23.60, 23.07, 22.86, 20.25, 16.97, 15.08 ppm.

*4.1.3. General procedure for synthesis of compounds **3a-3g***

Compound **2** (0.2 mmol) was added to 1.5 ml of dry CH_2Cl_2, 2 drops of DMF, and 0.6 mmol of oxalyl chloride, After being stirred under room temperature for 1 h, the reaction mixture was concentrated. Then anhydrous CH_2Cl_2 (2 mL), amine compounds (0.3 mmol) and DIEA (0.3 mmol) were added and the reaction was carried out at room temperature and monitored by TLC. Finally the reaction mixture was concentrated and purified by silica gel

Journal Pre-proofs
column chromatography to yield **3a-3g** (55%-92%).

*4.1.4. N-(maleimide-1-ethyl)-2-methylene-3-oxo-olean-12-en-28-amide (**3a**)* Yield 56%, white solid. HPLC: Purity 97.5%. HRMS (ESI Positive) m/z: calcd for $C_{37}H_{53}N_2O_4$ $[M+H]^+$: 589.4005; found:589.4006. ^{1}H NMR (400 MHz, $CDCl_3$) δ6.71(s, 2H), 6.16(s, 1H), 5.97(s, 1H), 5.42 (t, *J* = 3.4 Hz, 1H), 5.15(s, 1H), 3.78 – 3.59 (m, 5H), 3.06 (ddd, *J* = 13.3, 7.8, 4.2 Hz, 1H), 2.61 (d, *J* = 15.1 Hz, 1H), 2.51 (d, *J* = 12.5 Hz, 1H), 2.11 (d, *J* = 15.1 Hz, 1H), 1.15 (s, 3H), 1.11 (s, 3H), 1.04 (s, 3H), 0.91 (s, 3H), 0.89 (s, 6H), 0.73 (s, 3H) ppm. ^{13}C NMR (101 MHz, $CDCl_3$) δ 207.32, 178.52, 170.84, 144.88, 141.88, 134.25(2C), 123.79, 122.61, 58.43, 54.06, 46.75, 46.29, 45.95, 45.33, 42.12, 41.88, 39.22, 38.81, 37.36, 36.79, 34.16, 33.04, 32.28, 31.58, 30.78, 28.26, 27.28, 25.69, 23.70, 23.57, 23.47, 22.78, 20.13, 18.47, 16.41, 15.00 ppm.

*4.1.5. N-1-(2-(2-(2-azidoethoxy)ethoxy)ethoxy)ethyl-2-methylene-3-oxo-olean-12-en-28-amide (**3b**)* Yield 40%, white solid. HPLC: Purity 99.1%. mp: 55-58℃. HRMS (ESI Positive) m/z: calcd for $C_{39}H_{63}N_4O_5$ $[M+H]^+$ 667.4798; found: 667.4808. ^{1}H NMR (400 MHz, $CDCl_3$) δ 6.32 (s, 1H), 6.00 (s, 1H), 5.42 (s, 1H), 5.16 (s, 1H), 3.67(s, 8H), 3.53(s, 4H), 3.39(s, 2H), 2.62(m, 2H), 2.14 (d, *J* = 15.2 Hz, 1H), 1.19 (s, 3H), 1.14 (s, 3H), 1.07 (s, 3H), 0.92 (s, 9H), 0.84 (s, 3H) ppm. ^{13}C NMR (101 MHz, $CDCl_3$) δ 207.26, 177.97, 144.67, 141.90, 123.69, 122.46, 70.76, 70.66, 70.63, 70.30, 70.11, 69.72, 54.10, 50.68, 46.80, 46.66, 46.42, 45.91, 45.31, 42.28, 42.21, 39.30, 39.09, 36.74, 34.16, 33.02, 32.66, 31.80, 30.74, 28.26, 27.34, 25.57, 23.72, 23.60, 22.73, 20.14, 16.62, 15.01 ppm.

*4.1.6. N-propargyl-2-methylene-3-oxo-olean-12-en-28-amide (**3c**)* Yield 92%, white solid. HPLC: Purity 99.6%. mp: 135-140℃. HRMS (ESI Positive) m/z: calcd for $C_{34}H_{50}NO_2$ $[M+H]^+$ 504.3842; found: 504.3839. ^{1}H NMR (400 MHz, $CDCl_3$) δ 6.10 (t, *J* = 4.7 Hz, 1H), 6.00 (s, 1H), 5.47 (t, *J* = 3.3 Hz, 1H), 5.17 (s, 1H), 4.09 – 3.90 (m, 2H), 2.64 (d, *J* = 15.1 Hz, 1H), 2.58 (dd, *J* = 12.8, 3.3 Hz, 1H), 2.22 (t, *J* = 2.5 Hz, 1H), 2.15 (d, *J* = 15.0 Hz, 1H), 1.20 (s, 3H), 1.14 (s, 3H), 1.07 (s, 3H), 0.94 (s, 3H), 0.92(s, 3H),0.91(s, 3H), 0.86 (s, 3H) ppm. ^{13}C NMR (101 MHz, $CDCl_3$) δ 207.47, 178.06, 144.91, 142.01, 123.89, 122.98, 79.78, 71.76, 54.19, 50.94, 46.93, 46.71, 46.52, 46.06, 45.42, 42.37, 39.43, 36.87, 34.21, 33.12, 32.44, 31.84, 30.87, 29.48, 28.38, 27.38, 25.71, 24.01, 23.71, 23.69, 22.88, 20.25, 16.85, 15.15 ppm.

*4.1.7. N-allyl-2-methylene-3-oxo-olean-12-en-28-amide (**3d**)* Yield 56%, light yellow solid.

Journal Pre-proofs
HPLC: Purity 99.6%. mp: 121-125℃. HRMS (ESI Positive) m/z: calcd for $C_{34}H_{52}NO_2$ $[M+H]^+$ 506.3998; found: 506.3986. ^1H NMR (400 MHz, $CDCl_3$) δ 5.98 (dd, *J* = 8.5, 4.1 Hz, 2H), 5.84 (ddd, *J* = 16.1, 10.9, 5.8 Hz, 1H), 5.43 (t, 1H), 5.15 (dt, *J* = 13.1, 11.4 Hz, 3H), 4.01 (dt, *J* = 13.6, 5.7 Hz, 1H), 3.65 (dt, *J* = 10.4, 4.8 Hz, 1H), 2.63 (d, *J* = 15.2 Hz, 1H), 2.14 (d, *J* = 15.0 Hz, 1H), 1.20 (s, 3H), 1.14 (s, 3H), 1.07 (s, 3H), 0.94 (s, 3H), 0.92 (s, 3H),0.91(s, 3H), 0.82 (s, 3H) ppm. ^{13}C NMR (101 MHz, $CDCl_3$) δ 207.36, 178.08, 148.16, 145.14, 141.98, 134.50, 123.83, 122.67, 116.45, 54.18, 46.89, 46.83, 46.52, 46.02, 45.41, 42.48, 42.38, 42.15, 39.40, 36.85, 34.27, 33.11, 32.66, 31.83, 30.85, 28.38, 27.41, 25.70, 23.96, 23.69, 22.85, 20.24, 16.74, 15.11 ppm.

*4.1.8. N-phenyl-2-methylene-3-oxo-olean-12-en-28-amide (**3e**)* Yield 36%, gray solid. HPLC: Purity 95.6%. mp: 199-201℃. HRMS (ESI Positive) m/z: calcd for $C_{37}H_{52}NO_2$ $[M+H]^+$ 542.3998;found:542.3997. ^1H NMR (400 MHz, $CDCl_3$) δ 7.68 (s, 1H), 7.48 (d, *J* = 7.8 Hz, 2H), 7.30 (t, *J* = 7.9 Hz, 2H), 7.08 (t, *J* = 7.4 Hz, 1H), 5.99 (s, 1H), 5.59 (t, *J* = 3.3 Hz, 1H), 5.17 (s, 1H), 2.71 (dd, *J* = 12.4, 2.9 Hz, 1H), 2.65 (d, *J* = 15.1 Hz, 1H), 2.15 (d, *J* = 15.6 Hz, 1H), 1.23 (s, 3H), 1.12 (s, 3H), 1.04 (s, 3H), 0.94 (s, 3H), 0.92(s, 3H), 0.91 (s, 3H), 0.78 (s, 3H) ppm. ^{13}C NMR (101 MHz, $CDCl_3$) δ 207.29, 176.36, 145.12, 141.86, 138.01, 128.96 (2C), 124.13, 123.76, 123.02, 119.77(2C), 54.06, 47.26, 46.82, 46.75, 45.92, 45.31, 42.74, 42.43, 39.30, 36.73, 34.20, 32.98, 32.48, 31.73, 30.78, 28.26, 27.38, 25.60, 24.13, 23.75, 23.57, 22.72, 20.06, 16.62, 15.06 ppm.

*4.1.9. N-p-methoxyphenyl-2-methylene-3-oxo-olean-12-en-28-amide (**3f**)* Yield 45%, white solid.HPLC: Purity 96.7%. mp:200-203℃. HRMS (ESI Positive) m/z: calcd for $C_{38}H_{54}NO_3$ $[M+H]^+$ 572.4104; found: 572.4099. ^1H NMR (400 MHz, $CDCl_3$) δ 7.57 (s, 1H), 7.38 (d, *J* = 9.0 Hz, 2H), 6.84 (d, *J* = 9.0 Hz, 2H), 5.99 (s, 1H), 5.57 (t, *J* = 3.2 Hz, 1H), 5.17 (s, 1H), 3.78 (s, *J* = 3.1 Hz, 3H), 2.69 (dd, *J* = 13.1, 3.6 Hz, 1H), 2.64 (d, *J* = 15.1 Hz, 1H), 2.15 (d, *J* = 15.2 Hz, 1H), 1.23 (s, 3H), 1.13 (s, 3H), 1.04 (s, 3H), 0.95 (s,3H), 0.94 (s,3H), 0.91 (s, 3H), 0.79 (s, 3H) ppm. ^{13}C NMR (101 MHz, $CDCl_3$) δ 207.38, 176.22, 156.41, 145.29, 142.00, 131.35, 123.86, 123.03, 121.70(2C), 114.23(2C), 55.61, 54.21, 47.20, 46.95, 46.91, 46.05, 45.46, 42.85, 42.55, 39.45, 36.87, 34.35, 33.13, 32.64, 31.88, 30.92, 28.41, 27.52, 25.74, 24.21, 23.87, 23.73, 22.85, 20.21, 16.84, 15.18 ppm.

*4.1.10. N-o-methoxyphenyl-2-methylene-3-oxo-olean-12-en-28-amide (**3g**)* Yield 35%, gray solid. HPLC: Purity 99.7%. mp: 145-150℃. HRMS (ESI Positive) m/z: calcd for $C_{38}H_{54}NO_3$

Journal Pre-proofs
$[M+H]^+$ 572.4104; found: 572.4082. ^1H NMR (400 MHz, $CDCl_3$) δ 8.49 (dd, *J* = 8.0, 1.5 Hz, 1H), 8.43 (s, 1H), 7.01 (td, *J* = 7.7, 1.5 Hz, 1H), 6.93 (td, *J* = 7.8, 1.1 Hz, 1H), 6.86 (d, *J* = 8.0 Hz, 1H), 5.99 (s, 1H), 5.55 (t, *J* = 3.2 Hz, 1H), 5.16 (s, 1H), 3.89 (s, 3H), 2.75 (dd, *J* = 12.4, 2.9 Hz, 1H), 2.64 (d, *J* = 15.1 Hz, 1H), 2.15 (d, *J* = 15.1 Hz, 1H), 1.22 (s, 3H), 1.12 (s, 3H), 1.03 (s, 3H), 0.95 (s,3H), 0.94 (s,3H), 0.88 (s, 3H), 0.70 (s, 3H) ppm. ^{13}C NMR (101 MHz, $CDCl_3$) δ 207.47, 176.44, 148.10, 144.27, 142.11, 128.18, 123.79, 123.39, 123.37, 121.37, 119.76, 109.85, 55.72, 54.28, 48.01, 47.00, 46.09, 45.49, 42.70, 42.35, 39.45, 36.89, 36.22, 34.43, 33.19, 32.84, 31.90, 30.92, 28.40, 27.58, 25.85, 24.28, 23.80, 23.76, 22.86, 20.23, 16.12, 15.14 ppm.

*4.1.11.General procedure for synthesis of compounds **4a-4n***

To a solution of compound **3c** (100.0 mg, 0.20 mmol) in t-BuOH/H_2O (v:v 1:1, 4 mL), sodium ascorbate (32.0 mg, 0.16 mmol) and $CuSO_4 \cdot 5H_2O$ (20.2 mg, 0.08 mmol) were added at room temperature. To this mixture, aryl azide (1.0 mmol) was added and the reaction mixture was stirred at 35℃ for overnight. The crude mixture was extracted with CH_2Cl_2 (3 × 20 ml) and the combined organic layer was dried over Na_2SO_4 and purified through column chromatography to offer **4a–4n**.

*4.1.12. N-((1-phenyl-1H-1,2,3-triazol-4-yl)methyl)-2-methylene-3-oxo-olean-12-en-28-amide **(4a)*** Yield 60%,white solid. HPLC: Purity 95.6%. mp: 181-186℃. HRMS (ESI Positive) m/z: calcd for $C_{40}H_{55}N_4O_2$ $[M+H]^+$ 623.4325; found: 623.4304. ^1H NMR (400 MHz, $CDCl_3$) δ 8.02 (s, 1H), 7.72 (d, *J* = 7.6 Hz, 2H), 7.51 (t, *J* = 7.5 Hz, 2H), 7.44 (d, *J* = 7.3 Hz, 1H), 6.74 (s, 1H), 5.98 (s, 1H), 5.45 (s, 1H), 5.15 (s, 1H), 4.61 (dd, *J* = 14.8, 4.6 Hz, 1H), 4.48 (dd, *J* = 14.8, 4.9 Hz, 1H), 2.66 (d, *J* = 12.0 Hz, 1H), 2.61 (d, *J* = 15.2 Hz, 1H), 2.10 (d, *J* = 14.8 Hz, 1H), 1.16 (s, 3H), 1.11 (s, 3H), 1.02 (s, 3H), 0.91 (s, 6H), 0.80 (s, 3H), 0.54 (s, 3H) ppm. ^{13}C NMR (101 MHz, $CDCl_3$) δ 207.32, 178.33, 145.54, 144.38, 141.99, 137.14, 129.85(2C), 128.87, 123.79, 122.98, 121.00, 120.53(2C), 54.16, 53.55, 46.84, 46.64, 46.42, 45.97, 45.39, 42.23, 39.31, 36.80, 35.03, 34.24, 33.12, 32.83, 31.86, 30.84, 28.35, 27.40, 25.67, 23.91, 23.70, 23.59, 22.79, 20.16, 16.40, 14.97 ppm.

*4.1.13. N-((1-(2-fluorophenyl)-1H-1,2,3-triazol-4-yl)methyl)-2-methylene-3-oxo-olean-12-en-28-amide **(4b)*** Yield 48%,white solid. HPLC: Purity 99.3%. mp: 188-191℃. HRMS (ESI Positive) m/z: calcd for $C_{40}H_{54}FN_4O_2$ $[M+H]^+$ 641.4231; found: 641.4221. ^1H NMR (400 MHz, $CDCl_3$) δ 8.06 (s, 1H), 7.95-7.87 (m, 1H), 7.48-7.40 (m, 1H), 7.32 (t, *J* = 7.6 Hz, 2H),

Journal Pre-proofs
6.66 (s, 1H), 5.98 (s, 1H), 5.46 (s, 1H), 5.15 (s, 1H), 4.62 (dd, *J* = 14.9, 5.0 Hz, 1H), 4.51 (dd, *J* = 15.0, 5.1 Hz, 1H), 2.11 (d, *J* = 15.2 Hz, 1H), 1.17 (s, 3H), 1.11 (s, 3H), 1.03 (s, 3H), 0.91 (s, 6H), 0.83 (s, 3H) ppm. ^{13}C NMR (101 MHz, $CDCl_3$) δ 207.46, 178.40, 154.86, 152.37, 144.53, 142.07, 130.48 (d, *J* = 7.7 Hz), 125.39, 125.35, 125.04, 123.86, 123.11, 117.25 (d, *J* = 20.0 Hz), 54.24, 46.93, 46.75, 46.53, 46.05, 45.46, 42.39, 42.34, 39.39, 36.87, 35.07, 34.30, 33.17, 32.77, 31.91, 30.91, 29.86, 28.42, 27.45, 25.73, 24.03, 23.75, 23.67, 22.86, 20.24, 16.39, 15.03 ppm.

*4.1.14. N-((1-(4-fluorophenyl)-1H-1,2,3-triazol-4-yl)methyl)-2-methylene-3-oxo-olean-12-en-28-amide (**4c**)* Yield 48%,white solid. HPLC: Purity 97.8%. mp:189-193℃. HRMS (ESI Positive) m/z: calcd for $C_{40}H_{54}FN_4O_2$ $[M+H]^+$ 641.4231; found: 641.4210. ^{1}H NMR (400 MHz, $CDCl_3$) δ 7.98 (s, 1H), 7.74-7.66 (m, 2H), 7.25-7.18 (m, 2H), 6.69 (t, *J* = 5.4 Hz, 1H), 5.99 (s, 1H), 5.45 (t, *J* = 3.2 Hz, 1H), 5.16 (s, 1H), 4.61 (dd, *J* = 15.0, 5.4 Hz, 1H), 4.45 (dd, *J* = 15.0, 5.5 Hz, 1H), 2.11 (d, *J* = 15.2 Hz, 1H), 1.17 (s, 3H), 1.12 (s, 3H), 1.03 (s, 3H), 0.91 (s, 6H), 0.84 (s, 3H), 0.56 (s, 3H) ppm. ^{13}C NMR (101 MHz, $CDCl_3$) δ 207.22, 178.37, 162.46 (d, *J* = 248.8 Hz), 145.67, 144.34, 141.91, 133.37 (d, *J* = 3.1 Hz), 123.79, 122.91, 122.43 (2C,d, *J* = 8.6 Hz), 121.22, 116.76 (2C,d, *J* = 23.2 Hz), 54.09, 46.78, 46.58, 46.36, 45.93, 45.33, 42.17, 39.26, 36.77, 34.98, 34.18, 33.08, 32.76, 31.81, 30.79, 28.28, 27.34, 25.64, 23.85, 23.65, 23.54, 22.76, 20.11, 16.35, 14.94 ppm.

*4.1.15. N-((1-(2-chlorophenyl)-1H-1,2,3-triazol-4-yl)methyl)-2-methylene-3-oxo-olean-12-en-28-amide (**4d**)* Yield 45%, light green solid. HPLC: Purity 95.5%. mp: 178-183℃. HRMS (ESI Positive) m/z: calcd for $C_{40}H_{54}ClN_4O_2$ $[M+H]^+$ 657.3935;found:657.3925. ^{1}H NMR (400 MHz, $CDCl_3$) δ 8.01 (s, 1H), 7.62-7.55 (m, 2H), 7.49-7.40 (m, 2H), 6.69 (t, *J* = 5.2 Hz, 1H), 5.98 (s, 1H), 5.47 (t, *J* = 2.9 Hz, 1H), 5.16 (s, 1H), 4.62 (dd, *J* = 15.0, 5.3 Hz, 1H), 4.52 (dd, *J* = 15.1, 5.3 Hz, 1H), 2.11 (d, *J* = 15.4 Hz, 1H), 1.18 (s, 3H), 1.12 (s, 3H), 1.04 (s, 3H), 0.91 (s, 6H), 0.87 (s, 3H), 0.62 (s, 3H) ppm. ^{13}C NMR (101 MHz, $CDCl_3$) δ 207.41, 178.51, 144.63, 144.56, 142.04, 135.03, 131.00, 130.92, 128.68, 128.03, 127.81, 124.81, 123.84, 123.09, 54.22, 46.92, 46.79, 46.49, 46.05, 45.45, 42.33, 42.30, 39.39, 36.87, 35.18, 34.30, 33.14, 32.70, 31.87, 30.88, 28.38, 27.41, 25.71, 24.08, 23.72, 23.68, 22.86, 20.24, 16.52, 15.13 ppm.

*4.1.16. N-((1-(4-chlorophenyl)-1H-1,2,3-triazol-4-yl)methyl)-2-methylene-3-oxo-olean-12-en-28-amide (**4e**)* Yield 59%, white solid. HPLC: Purity 97.9%. mp: 203-207℃. HRMS (ESI Positive) m/z: calcd for $C_{40}H_{54}ClN_4O_2$ $[M+H]^+$ 657.3935; found: 657.3924. ^{1}H NMR (400

Journal Pre-proofs
MHz, $CDCl_3$) δ 7.99 (s, 1H), 7.67 (d, *J* = 8.8 Hz, 2H), 7.49 (d, *J* = 8.8 Hz, 2H), 6.66 (t, *J* = 4.8 Hz, 1H), 5.99 (t, *J* = 2.0 Hz, 1H), 5.45 (t, *J* = 3.3 Hz, 1H), 5.16 (s, 1H), 4.60 (dd, *J* = 15.0, 5.4 Hz, 1H), 4.45 (dd, *J* = 15.0, 5.5 Hz, 1H), 2.67-2.58 (m, 2H), 2.11 (d, *J* = 15.1 Hz, 1H), 1.17 (s, 3H), 1.11 (s, 3H), 1.03 (s, 3H), 0.90 (d, *J* = 1.8 Hz, 6H), 0.83 (s, 3H) ppm. ^{13}C NMR (101 MHz, $CDCl_3$) δ 207.31, 178.48, 145.83, 144.43, 141.97, 135.63, 134.68, 130.04(2C), 123.86, 123.00, 121.69(2C), 121.03, 54.17, 46.86, 46.65, 46.44, 46.00, 45.40, 42.25, 39.32, 36.83, 35.03, 34.23, 33.12, 32.80, 31.86, 30.85, 28.33, 27.40, 25.68, 23.96, 23.70, 23.61, 22.82, 20.17, 16.42, 15.00, 14.24 ppm.

*4.1.17. N-((1-(2-nitrophenyl)-1H-1,2,3-triazol-4-yl)methyl)-2-methylene-3-oxo-olean-12-en-28-amide (**4f**)* Yield 65%,light yellow solid. HPLC: Purity 97.5%. mp:188-191℃. HRMS (ESI Positive) m/z: calcd for $C_{40}H_{54}N_5O_4$ $[M+H]^+$ 668.4176; found: 668.4166. ^{1}H NMR (400 MHz, $CDCl_3$) δ 8.07 (d, *J* = 8.0 Hz, 1H), 7.78 (t, *J* = 7.6 Hz, 1H), 7.70 (t, *J* = 7.8 Hz, 1H), 7.59 (d, *J* = 7.7 Hz, 1H), 6.72 (t, *J* = 4.8 Hz, 1H), 5.98 (s, 1H), 5.47 (s, 1H), 5.16 (s, 1H), 4.62 (dd, *J* = 15.0, 5.2 Hz, 1H), 4.48 (dd, *J* = 15.0, 5.0 Hz, 1H), 2.63 (dd, *J* = 9.5, 5.7 Hz, 2H), 2.12 (d, *J* = 15.0 Hz, 1H), 1.18 (s, 3H), 1.12 (s, 3H), 1.04 (s, 3H), 0.91 (s, 6H), 0.89-0.88 (m, 3H), 0.66 (s, 3H) ppm. ^{13}C NMR (101 MHz, $CDCl_3$) δ 207.35, 178.56, 145.36, 144.54, 144.43, 141.97, 133.75, 130.81, 130.22, 127.73, 125.64, 124.30, 123.73, 123.02, 54.12, 46.81, 46.68, 46.37, 45.95, 45.37, 42.21, 42.14, 39.31, 36.78, 35.06, 34.19, 33.05, 32.59, 31.74, 30.78, 28.28, 27.32, 25.64, 23.97, 23.63, 23.57, 22.78, 20.14, 16.45, 15.00 ppm.

*4.1.18. N-((1-(4-nitrophenyl)-1H-1,2,3-triazol-4-yl)methyl)-2-methylene-3-oxo-olean-12-en-28-amide (**4g**)* Yield 77%,light yellow solid. HPLC: Purity 98.3%. mp: 216-225℃. HRMS (ESI Positive) m/z: calcd for $C_{40}H_{54}N_5O_4$ $[M+H]^+$ 668.4176; found: 668.4167. ^{1}H NMR (400 MHz, $CDCl_3$) δ 8.42 (d, *J* = 9.1 Hz, 2H), 8.16 (s, 1H), 7.97 (d, *J* = 9.1 Hz, 2H), 6.68 (t, *J* = 5.5 Hz, 1H), 5.99 (t, *J* = 2.1 Hz, 1H), 5.46 (t, *J* = 3.2 Hz, 1H), 5.17 (s, 1H), 4.63 (dd, *J* = 15.0, 5.5 Hz, 1H), 4.45 (dd, *J* = 15.0, 5.4 Hz, 1H), 2.66-2.58 (m, 2H), 2.12 (d, *J* = 15.2 Hz, 1H), 1.18 (s, 3H), 1.12 (s, 3H), 1.02 (s, 3H), 0.91 (s, 6H),0.90 (s, 6H), 0.85 (s, 3H), 0.59 (s, 3H) ppm. ^{13}C NMR (101 MHz, $CDCl_3$) δ 207.15, 178.58, 147.25, 146.45, 144.37, 141.86, 141.22, 125.57(2C), 123.80, 122.93, 121.16, 120.47(2C), 54.05, 46.77, 46.54, 46.38, 45.92, 45.31, 42.19, 42.15, 39.25, 36.76, 34.97, 34.14, 33.03, 32.72, 31.77, 30.77, 28.23, 27.32, 25.63, 23.89, 23.61, 23.54, 22.76, 20.09, 16.36, 14.94 ppm.

4.1.19. N-((1-(2-methylphenyl)-1H-1,2,3-triazol-4-yl)methyl)-2-methylene-3-oxo-olean-12-en-

Journal Pre-proofs

*28-amide (**4h**)* Yield 41%,yellow solid. HPLC: Purity 96.4%. mp: 170-175℃. HRMS (ESI Positive) m/z: calcd for $C_{41}H_{57}N_4O_2$ $[M+H]^+$ 637.4482; found: 637.4467. ^{1}H NMR (400 MHz, $CDCl_3$) δ 7.76 (s, 1H), 7.43-7.34 (m, 2H), 7.34-7.29 (m, 2H), 6.71 (t, *J* = 5.4 Hz, 1H), 5.99 (s, 1H), 5.47 (t, *J* = 3.1 Hz, 1H), 5.16 (s, 1H), 4.62 (dd, *J* = 15.0, 5.4 Hz, 1H), 4.50 (dd, *J* = 15.0, 5.3 Hz, 1H), 2.69 – 2.60 (m, 2H), 2.22 (s, 3H), 2.12 (d, *J* = 15.3 Hz, 1H), 1.18 (s, 3H), 1.12 (s, 3H), 1.05 (s, 3H), 0.91 (s, 6H), 0.87 (s, 3H), 0.64 (s, 3H) ppm. ^{13}C NMR (101 MHz, $CDCl_3$) δ 207.25, 178.33, 144.37, 141.86, 140.20, 136.42, 133.41, 131.54, 129.85, 126.83, 125.85, 124.12, 123.73, 122.92, 54.05, 46.75, 46.61, 46.33, 45.90, 45.29, 42.16, 42.11, 39.23, 36.72, 35.04, 34.13, 33.00, 32.58, 31.73, 30.73, 28.22, 27.27, 25.57, 23.89, 23.57, 23.52, 22.71, 20.07, 17.90, 16.44, 14.97 ppm.

*4.1.20. N-((1-(4-methylphenyl)-1H-1,2,3-triazol-4-yl)methyl)-2-methylene-3-oxo-olean-12-en-28-amide (**4i**)* Yield 51%,white solid. HPLC: Purity 99.4%. mp: 172-177℃. HRMS (ESI Positive) m/z: calcd for $C_{41}H_{57}N_4O_2$ $[M+H]^+$ 637.4482; found:637.4465. ^{1}H NMR (400 MHz, $CDCl_3$) δ 7.95 (s, 1H), 7.58 (d, *J* = 8.4 Hz, 2H), 7.30 (d, *J* = 8.3 Hz, 2H), 6.68 (t, 1H), 5.98 (s, 1H), 5.45 (t, *J* = 3.2 Hz, 1H), 5.15 (s, 1H), 4.60 (dd, *J* = 14.9, 5.2 Hz, 1H), 4.47 (dd, *J* = 14.9, 5.4 Hz, 1H), 2.69-2.56 (m, 2H), 2.41 (s, 3H), 2.10 (d, *J* = 15.1 Hz, 1H), 1.16 (s, 3H), 1.11 (s, 3H), 1.02 (s, 3H), 0.91 (s, 6H), 0.81 (s, 3H), 0.54 (s, 3H) ppm. ^{13}C NMR (101 MHz, $CDCl_3$) δ 207.35, 178.30, 145.35, 144.34, 141.96, 138.98, 134.83, 130.30(2C), 123.82, 122.95, 120.98, 120.43(2C), 54.12, 46.80, 46.61, 46.38, 45.94, 45.36, 42.19, 39.27, 36.77, 35.00, 34.22, 33.11, 32.79, 31.83, 31.67, 30.83, 28.34, 27.37, 25.65, 23.87, 23.68, 23.57, 22.76, 22.74, 21.17, 20.14, 16.37, 14.95, 14.22 ppm.

*4.1.21. N-((1-(2-methoxylphenyl)-1H-1,2,3-triazol-4-yl)methyl)-2-methylene-3-oxo-olean-12-en-28-amide (**4j**)* Yield 57%,light yellow solid. HPLC: Purity 96.8%. mp: 146-152℃. HRMS (ESI Positive) m/z: calcd for $C_{41}H_{57}N_4O_3$ $[M+H]^+$ 653.4431; found:653.4417. ^{1}H NMR (400 MHz, $CDCl_3$) δ 8.09 (s, 1H), 7.75 (d, *J* = 7.0 Hz, 1H), 7.46-7.39 (m, 1H), 7.09 (t, *J* = 7.5 Hz, 2H), 6.70 (t, *J* = 5.1 Hz, 1H), 5.98 (s, 1H), 5.46 (t, *J* = 3.0 Hz, 1H), 5.15 (s, 1H), 4.61 (dd, *J* = 15.0, 5.3 Hz, 1H), 4.51 (dd, *J* = 14.9, 5.3 Hz, 1H), 3.88 (s, 3H), 2.64 (m, 2H), 2.11 (d, *J* = 15.0 Hz, 1H), 1.17 (s, 3H), 1.11 (s, 3H), 1.03 (s, 3H), 0.91 (s, 6H), 0.83 (s, 3H), 0.56 (s, 3H) ppm. ^{13}C NMR (101 MHz, $CDCl_3$) δ 207.33, 178.16, 151.07, 144.34, 144.07, 141.95, 130.16, 126.31, 125.38, 124.64, 123.75, 123.00, 121.21, 112.28, 55.96, 54.12, 46.80, 46.63, 46.37, 45.93, 45.35, 42.22, 42.20, 39.26, 36.76, 35.03, 34.22, 33.08, 32.67, 31.83, 30.80, 28.30, 27.35, 25.62, 23.90, 23.65, 23.56, 22.76, 20.15, 16.30, 14.96 ppm.

*4.1.22. N-((1-(3-methoxylphenyl)-1H-1,2,3-triazol-4-yl)methyl)-2-methylene-3-oxo-olean-12-en-28-amide (**4k**)* Yield 43%,red solid. HPLC: Purity 98.8%. mp:118-124℃. HRMS (ESI Positive) m/z: calcd for $C_{41}H_{57}N_4O_3$ $[M+H]^+$ 653.4431; found: 653.4417. ^{1}H NMR (400 MHz, $CDCl_3$) δ 7.99 (s, 1H), 7.40 (t, *J* = 8.1 Hz, 1H), 7.31 (s, 1H), 7.24 (d, *J* = 7.9 Hz, 1H), 6.96 (dd, *J* = 8.3, 2.0 Hz, 1H), 6.65 (s, 1H), 5.98 (s, 1H), 5.45 (s, 1H), 5.15 (s, 1H), 4.60 (dd, *J* = 14.9, 4.8 Hz, 1H), 4.47 (dd, *J* = 14.9, 4.8 Hz, 1H), 3.87 (s, 3H), 2.68-2.57 (m, 2H), 2.10 (d, *J* = 15.0 Hz, 1H), 1.16 (s, 3H), 1.11 (s, 3H), 1.02 (s, 3H), 0.91 (s, 6H), 0.82 (s, 3H), 0.55 (s, 3H) ppm. ^{13}C NMR (101 MHz, $CDCl_3$) δ 207.37, 178.33, 160.71, 145.43, 144.34, 141.96, 138.10, 130.61, 123.80, 122.95, 121.09, 114.62, 112.42, 106.41, 55.71, 54.12, 46.81, 46.60, 46.39, 45.94, 45.35, 42.20, 39.27, 36.77, 34.95, 34.20, 33.09, 32.79, 31.83, 30.81, 28.32, 27.36, 25.63, 23.89, 23.66, 23.56, 22.74, 20.13, 16.37, 14.94, 14.28 ppm.

*4.1.23. N-((1-(4-methoxylphenyl)-1H-1,2,3-triazol-4-yl)methyl)-2-methylene-3-oxo-olean-12-en-28-amide (**4l**)* Yield 57%,white solid. HPLC: Purity 99.8%. mp: 115-121℃. HRMS (ESI Positive) m/z: calcd for $C_{41}H_{57}N_4O_3$ $[M+H]^+$ 653.4431; found: 653.4417. ^{1}H NMR (400 MHz, $CDCl_3$) δ 7.92 (s, 1H), 7.61 (d, *J* = 8.6 Hz, 2H), 7.00 (d, *J* = 8.6 Hz, 2H), 6.71 (s, 1H), 5.98 (s, 1H), 5.45 (s, 1H), 5.15 (s, 1H), 4.59 (dd, *J* = 14.9, 5.0 Hz, 1H), 4.47 (dd, *J* = 14.9, 5.2 Hz, 1H), 3.85 (s, 3H), 2.63 (m, 2H), 2.11 (d, *J* = 15.0 Hz, 1H), 1.16 (s, 3H), 1.11 (s, 3H), 1.02 (s, 3H), 0.91 (s, 6H), 0.82 (s, 3H), 0.55 (s, 3H) ppm. ^{13}C NMR (101 MHz, $CDCl_3$) δ 207.32, 178.30, 159.94, 145.27, 144.36, 141.96, 130.55, 123.78, 122.96, 122.13(2C), 121.06, 114.84, 55.71, 54.13, 53.51, 46.81, 46.62, 46.39, 45.95, 45.37, 42.21, 39.28, 36.78, 35.00, 34.21, 33.09, 32.76, 31.83, 30.81, 28.32, 27.37, 25.64, 23.90, 23.67, 23.57, 22.76, 20.14, 16.37, 14.97 ppm.

*4.1.24. N-((1-(2-methyl-4-nitrophenyl)-1H-1,2,3-triazol-4-yl)methyl)-2-methylene-3-oxo-olean-12-en-28-amide (**4m**)* Yield 72%,light yellow solid. HPLC: Purity 98.3%. mp: 178-183℃. HRMS (ESI Positive) m/z: calcd for $C_{41}H_{56}N_5O_4$ $[M+H]^+$ 682.4332;found: 682.4320. ^{1}H NMR (400 MHz, $CDCl_3$) δ 8.28 (d, *J* = 1.9 Hz, 1H), 8.20 (dd, *J* = 8.6, 2.0 Hz, 1H), 7.91 (s, 1H), 7.55 (d, *J* = 8.6 Hz, 1H), 6.73 (s, 1H), 5.99 (s, 1H), 5.48 (s, 1H), 5.16 (s, 1H), 4.63 (dd, 1H), 4.49 (dd, *J* = 11.2 Hz, 1H), 2.63 (m, 2H), 2.41 (s, 3H), 2.13 (d, *J* = 15.0 Hz, 1H), 1.99 (dd, *J* = 8.6, 2.5 Hz, 2H), 1.19 (s, 3H), 1.13 (s, 3H), 1.05 (s, 3H), 0.92 (s, 3H),0.91 (s, 3H), 0.89 (s, 3H), 0.64 (s, 3H) ppm. ^{13}C NMR (101 MHz, $CDCl_3$) δ 207.21, 178.67, 148.01, 144.47, 141.88, 141.14, 135.16, 126.91, 126.73, 123.85, 123.01, 122.27,

Journal Pre-proofs
54.10, 46.82, 46.65, 46.42, 45.97, 45.35, 42.25, 42.16, 39.31, 36.81, 35.08, 34.18, 33.05, 32.66, 31.81, 30.80, 28.27, 27.33, 25.66, 23.98, 23.64, 23.61, 22.81, 20.14, 18.73, 16.52, 15.05 ppm.

*4.1.25. N-((1-(2,3-difluorophenyl)-1H-1,2,3-triazol-4-yl)methyl)-2-methylene-3-oxo-olean-12-en-28-amide (**4n**)* Yield 66%,light yellow solid. HPLC: Purity 96.4%. mp:118-124℃. HRMS (ESI Positive) m/z: calcd for $C_{40}H_{53}F_2N_4O_2$ $[M+H]^+$ 659.4137;found: 659.4125. ^1H NMR (400 MHz, $CDCl_3$) δ 8.13 (d, *J* = 2.9 Hz, 1H), 7.73 (ddd, *J* = 8.7, 5.8, 3.1 Hz, 1H), 7.28 (dt, *J* = 10.1, 4.1 Hz, 1H), 7.17 – 7.10 (m, 1H), 6.73 (t, *J* = 5.4 Hz, 1H), 5.98 (t, *J* = 2.0 Hz, 1H), 5.45 (t, *J* = 3.3 Hz, 1H), 5.15 (s, 1H), 4.62 (dd, *J* = 15.0, 5.4 Hz, 1H), 4.50 (dd, *J* = 15.0, 5.4 Hz, 1H), 2.65 (dd, *J* = 21.9, 9.1 Hz, 2H), 2.11 (d, *J* = 14.8 Hz, 1H), 1.96 (dd, *J* = 8.8, 3.4 Hz, 2H), 1.17 (s, 3H), 1.12 (s, 3H), 1.03 (s, 3H), 0.91 (s, 6H), 0.84 (s, 3H), 0.56 (s, 3H) ppm. ^{13}C NMR (101 MHz, $CDCl_3$) δ 207.21, 178.25, 171.09, 158.59 (dd, *J* = 245.8, 2.4 Hz), 149.22 (dd, *J* = 247.2, 3.2 Hz), 145.46, 144.30, 141.85, 125.70 (dd, *J* = 12.1, 10.7 Hz), 123.77, 122.85, 118.16 (dd, *J* = 22.9, 9.0 Hz), 116.61 (dd, *J* = 24.0, 8.0 Hz), 111.61 (d, *J* = 28.3 Hz), 60.35, 54.02, 46.71, 46.51, 46.31, 45.85, 45.25, 42.11, 39.17, 36.68, 34.82, 34.09, 32.98, 32.62, 31.71, 30.70, 28.20, 27.24, 25.54, 23.78, 23.54, 23.46, 22.65, 21.01, 20.03, 16.19, 14.82, 14.18 ppm.

4.2.Biological assays

4.2.1. Cell Culture

MCF-7, HeLa and HepG2 cells were cultured in DMEM growth medium, supplemented with 10% FBS and 1% Penicillian-Streptomycin. All of the cell lines were grown at 37℃ in a 5% CO_2 atmosphere.

4.2.2. MTT assay

The compounds were dissolved in DMSO and diluted to the required concentration with the culture medium when used. The cells harvested from the exponential phase were equivalently seeded into a 96-well plate (3000 cells/well) and treated with or without different concentrations of the test compounds for 48 h. The MTT (20 μL, 5 mg/mL) was added into each well, the cells were incubated for additional 4 h, and the resulting formazan crystals were dissolved in 200 μL of DMSO and the absorbance was read at 570 nm. Experiments were conducted in triplicate.

4.2.3. Apoptosis analysis

MCF-7 cells were incubated in six-well plates(3.5×10^5 cells/well) and treated with **3d** at concentrations of 0,2,4,8 μM for 24 h, respectively. The cells were collected, washed with PBS, and stained with FITC-Annexin-V and PI and incubated for 15 min. Apoptosis was determined by flow cytometry. Annexin-V positive, propidium iodide negative cells were considered early apoptotic and Annexin-V positive, propidium iodide positive cells were considered late apoptotic.

4.2.4. Cell cycle analysis

MCF-7 cells were treated with **3d** at concentrations of 0,2,4,8 μM for 24 h, respectively. The cells were harvested, fixed with 75% ethanol for 4 h at -20℃, and incubated with PI/RNase staining buffer for 30 min at room temperature. The DNA content in different groups of cells was assessed by flow cytometry.

4.2.5. Cell migration scratch assay

For wound healing assay, 2 ml MCF-7 or HeLa cells with a density of 5×10^5 cells/well were placed in 6-well plate and incubated at 37 ℃in a humidified atmosphere with 5% CO_2 for 12-24 h and grown to confluency. Then we used 20 μL pipette to scratch cell monolayers to create a cell-free zone. Washed each well 3 times with PBS buffer and incubated using serum-free media or **3d** to each well, and then incubated at 37 ℃ with 5% CO_2 for 24 h. Photographed at 0 h, 24 h under the microscope to observe cell migration.

4.2.6 .Network pharmacological analysis

The Pharma DB database in Discovery Studio software was used to predict the target of compound **3d**, and the result with a FitValue greater than 0.9 was selected. In order to further determine the most likely target protein, we imported the predicted protein target into the string database(https://string-db.org/) to define species for humans, got the protein interaction relationship, saved the results in TSV format, and import Cytoscape 3.6.0 statistical software to draw interaction networks. First analyzed the protein interaction network as a whole, then used the cytohubba plug-in in Cytoscape statistical software to determine the 15 most important protein interaction relationships, and selected the maximum cluster centrality (MCC) for the calculation method. KEGG analysis was performed on the protein input the

DAVID 6.8(https://david.ncifcrf.gov) .

4.2.7. Western blotting analysis

MCF-7 Cells at a density of 4 ×105 cells/3 mL were seeded onto 6-well plates. After incubation for 24 h, 3d at various concentrations were added. After treatment, cells were collected and lysed in RIPA buffer (50 mM Tris-HCl, pH 8.0, 150 mM NaCl, 1% NP-40,0.5% sodium deoxycholate, 0.1% SDS), and centrifuged at 13,000 r for 15 min in the 4 ℃ centrifuge. Supernatants were collected, and the total protein concentration was quantified with a bicinchoninic acid (BCA) assay kit. The protein concentration was determined, equal amounts of proteins were loaded onto SDS-PAGE gels, and separated proteins were transferred to PVDF membranes. After blocking with 5% BSA at room temperature for 2 h, the membranes were incubated with primary antibodies against AKT,p-AKT,mTOR and p-mTOR, a monoclonal antibody against β-actin was used as a protein loading control. The membranes were washed three times with TBST buffer for 30 min, 10 min at a time, then incubated with HRP-conjugated secondary antibody for 2 h. After being washed with the TBST buffer again, membranes were scanned with the Odyssey Infrared Imaging System.

Conflicts of interest

The authors declare that there are no conflicts of interest.

Acknowledgements

This study was supported by the National Natural Science Foundation of China (Grant No. 21506024) and Natural Science Foundation of Liaoning Province (2019-MS-060).

Reference

[1] J. Pollier, A. Goossens, Oleanolic acid, Phytochemistry. 77 (2012) 10–15. https://doi.org/10.1016/j.phytochem.2011.12.022.

[2] X.L. Wan, Y.F. Lu, S.F. Xu, Q. Wu, J. Liu, Oeanolic acid protects against the hepatotoxicity of D-galactosame plus endotoxin in mice, Biomed. Pharmacother. 93 (2017) 1040–1046. https://doi.org/10.1016/j.biopha.2017.07.045.

[3] J. Liu, Y.F. Lu, Q. Wu, S.F. Xu, F.G. Shi, C.D. Klaassen, Oleanolic acid reprograms the liver to protect against hepatotoxicants, but is hepatotoxic at high doses, Liver Int. 39 (2019) 427–439. https://doi.org/10.1111/liv.13940.

[4] M. Masullo, C. Pizza, S. Piacente, Oleanane derivatives for pharmaceutical use: a patent review (2000-2016), Expert Opin. Ther. Pat. 27 (2017) 237–255. https://doi.org/10.1080/13543776.2017.1253680.

[5] M.K. Shanmugam, X. Dai, A.P. Kumar, B.K.H. Tan, G. Sethi, A. Bishayee, Oleanolic acid and its synthetic derivatives for the prevention and therapy of cancer: Preclinical and clinical evidence, Cancer Lett. 346 (2014) 206–216. https://doi.org/10.1016/j.canlet.2014.01.016.

[6] M.W. Pertino, C. Lopez, C. Theoduloz, G. Schmeda-Hirschmann, 1,2,3-triazole-substituted oleanolic acid derivatives: Synthesis and antiproliferative activity, Molecules. 18 (2013) 7661–7674. https://doi.org/10.3390/molecules18077661.

[7] H.E. Elsayed, M.R. Akl, H.Y. Ebrahim, A.A. Sallam, E.G. Haggag, A.M. Kamal, K.A. El Sayed, Discovery, optimization, and pharmacophore modeling of oleanolic acid and analogues as breast cancer cell migration and invasion inhibitors through targeting Brk/Paxillin/Rac1 axis, Chem. Biol. Drug Des. 85 (2015) 231–243. https://doi.org/10.1111/cbdd.12380.

[8] J.J. Ramírez-Espinosa, M.Y. Rios, P. Paoli, V. Flores-Morales, G. Camici, V.D. La Rosa-Lugo, S. Hidalgo-Figueroa, G. Navarrete-Vázquez, S. Estrada-Soto, Synthesis of oleanolic acid derivatives: In vitro, in vivo and in silico studies for PTP-1B inhibition, Eur. J. Med. Chem. 87 (2014) 316–327. https://doi.org/10.1016/j.ejmech.2014.09.036.

[9] X. Han, L.L. Si, Y.Y. Shi, Z.B. Fan, S.X. Wang, Z.Y. Tian, M. Li, J.Q. Sun, P.X. Jiao, F.X. Ran, Y.M. Zhang, D.M. Zhou, S.L. Xiao, Synthesis and in vitro anti-influenza virus evaluation of novel sialic acid (C-5 and C-9)-pentacyclic triterpene derivatives, Molecules. 22 (2017) 1–17. https://doi.org/10.3390/molecules22071018.

[10] L. Fu, Q.X. Lin, E.O. Onyango, K.T. Liby, M.B. Sporn, G.W. Gribble, Design, synthesis, and biological activity of second-generation synthetic oleanane triterpenoids, Org. Biomol. Chem. 15 (2017) 6001–6005. https://doi.org/10.1039/c7ob01420a.

[11] L.X. Rui, S.Y. Shu, W.J. Jun, C.Z. Mo, S.Z. Wu, L.S. Min, L. Yuan, P.J. Yong, S.Z. Cheng, W.S. Sheng, T.Z. Yao, The dual induction of apoptosis and autophagy by SZC014, a synthetic oleanolic acid derivative, in gastric cancer cells via NF-κB pathway, Tumor Biol. 37 (2016) 5133–5144. https://doi.org/10.1007/s13277-015-4293-2.

[12] L. Gao, Z. Xu, Y. Wang, B. Sun, Z. Song, B. Yang, X. Liu, Y. Lin, J. Peng, G. Han, S. Wang, Z. Tang, Anticancer effect of SZC017, a novel derivative of oleanolic acid on human gastric cancer

cells, Oncol. Rep. 35 (2016) 1101–1108. https://doi.org/10.3892/or.2015.4447.

[13] Y. Song, L. Gao, Z. Tang, H. Li, B. Sun, P. Chu, E. Qaed, X. Ma, J. Peng, S. Wang, M. Hu, Z. Tang, Anticancer effect of SZC015 on pancreatic cancer via mitochondria-dependent apoptosis and the constitutive suppression of activated nuclear factor κB and STAT3 in vitro and in vivo, J. Cell. Physiol. 234 (2018) 777–788. https://doi.org/10.1002/jcp.26892.

[14] L. Gao, Y. Wang, Z. Xu, X. Li, J. Wu, S. Liu, P. Chu, Z. Sun, B. Sun, Y. Lin, J. Peng, G. Han, S. Wang, Z. Tang, SZC017, a novel oleanolic acid derivative, induces apoptosis and autophagy in human breast cancer cells, Apoptosis. 20 (2015) 1636–1650. https://doi.org/10.1007/s10495-015-1179-0.

[15] P. Chu, H. Li, R. Luo, A. Ahsan, E. Qaed, A. Shopit, X. Ma, Y. Lin, J. Peng, J. Zhang, S. Wang, Z. Tang, Oleanolic acid derivative SZC014 inhibit cell proliferation and induce apoptosis of human breast cancer cells in a ROS-dependent way, Neoplasma. 64 (2017) 681–692. https://doi.org/10.4149/neo_2017_505.

[16] Y. Song, L. Kong, B. Sun, L. Gao, P. Chu, A. Ahsan, E. Qaed, Y. Lin, J. Peng, X. Ma, J. Zhang, S. Wang, Z. Tang, Induction of autophagy by an oleanolic acid derivative, SZC017, promotes ROS-dependent apoptosis through Akt and JAK2/STAT3 signaling pathway in human lung cancer cells, Cell Biol. Int. 41 (2017) 1367–1378. https://doi.org/10.1002/cbin.10868.

[17] B. Sun, L. Gao, A. Ahsan, P. Chu, Y. Song, H. Li, Z. Zhang, Y. Lin, J. Peng, Z. Song, S. Wang, Z. Tang, Anticancer effect of SZC015 on lung cancer cells through ROS-dependent apoptosis and autophagy induction mechanisms in vitro, Int. Immunopharmacol. 40 (2016) 400–409. https://doi.org/10.1016/j.intimp.2016.09.026.

[18] M.B. Sporn, K.T. Liby, M.M. Yore, L. Fu, J.M. Lopchuk, G.W. Gribble, New synthetic triterpenoids: Potent agents for prevention and treatment of tissue injury caused by inflammatory and oxidative stress, J. Nat. Prod. 74 (2011) 537–545. https://doi.org/10.1021/np100826q.

[19] T. Honda, G.W. Gribble, N. Suh, H.J. Finlay, B.A. V. Rounds, L. Bore, F.G. Favaloro, Y. Wang, M.B. Sporn, Novel synthetic oleanane and ursane triterpenoids with various enone functionalities in ring A as inhibitors of nitric oxide production in mouse macrophages, J. Med. Chem. 43 (2000) 1866–1877. https://doi.org/10.1021/jm000008j.

[20] T. Honda, B. V. Rounds, L. Bore, H.J. Finlay, F.G. Favaloro, N. Suh, Y. Wang, M.B. Sporn, G.W. Gribble, Synthetic oleanane and ursane triterpenoids with modified rings A and C: A series of

highly active inhibitors of nitric oxide production in mouse macrophages, J. Med. Chem. 43 (2000) 4233–4246. https://doi.org/10.1021/jm0002230.

[21] M.H.L. Wong, H.K. Bryan, I.M. Copple, R.E. Jenkins, P.H. Chiu, J. Bibby, N.G. Berry, N.R. Kitteringham, C.E. Goldring, P.M. O'Neill, B.K. Park, Design and Synthesis of Irreversible Analogues of Bardoxolone Methyl for the Identification of Pharmacologically Relevant Targets and Interaction Sites, J. Med. Chem. 59 (2016) 2396–2409. https://doi.org/10.1021/acs.jmedchem.5b01292.

[22] A. Cleasby, J. Yon, P.J. Day, C. Richardson, I.J. Tickle, P.A. Williams, J.F. Callahan, R. Carr, N. Concha, J.K. Kerns, H. Qi, T. Sweitzer, P. Ward, T.G. Davies, Structure of the BTB domain of Keap1 and its interaction with the triterpenoid antagonist CDDO, PLoS One. 9 (2014) 15–21. https://doi.org/10.1371/journal.pone.0098896.

[23] M. Gehringer, S.A. Laufer, Emerging and Re-Emerging Warheads for Targeted Covalent Inhibitors: Applications in Medicinal Chemistry and Chemical Biology, J. Med. Chem. 62 (2019) 5673–5724. https://doi.org/10.1021/acs.jmedchem.8b01153.

[24] S. Ray, A.S. Murkin, New Electrophiles and Strategies for Mechanism-Based and Targeted Covalent Inhibitor Design, Biochemistry. (2019). https://doi.org/10.1021/acs.biochem.9b00293.

[25] M. Hossain, U. Das, J.R. Dimmock, Recent advances in α,β-unsaturated carbonyl compounds as mitochondrial toxins, Eur. J. Med. Chem. 183 (2019). https://doi.org/10.1016/j.ejmech.2019.111687.

[26] E.H. Krenske, R.C. Petter, K.N. Houk, Kinetics and Thermodynamics of Reversible Thiol Additions to Mono- and Diactivated Michael Acceptors: Implications for the Design of Drugs That Bind Covalently to Cysteines, J. Org. Chem. 81 (2016) 11726–11733. https://doi.org/10.1021/acs.joc.6b02188.

[27] G. Akçay, M.A. Belmonte, B. Aquila, C. Chuaqui, A.W. Hird, M.L. Lamb, P.B. Rawlins, N. Su, S. Tentarelli, N.P. Grimster, Q. Su, Inhibition of Mcl-1 through covalent modification of a noncatalytic lysine side chain, Nat. Chem. Biol. 12 (2016) 931–936. https://doi.org/10.1038/nchembio.2174.

[28] D. De Zeeuw, T. Akizawa, Bardoxolone methyl in type 2 diabetes and stage 4 chronic kidney disease, N. Engl. J. Med. 369 (2013) 2492–2503. https://doi.org/10.1056/NEJMoa1306033.

[29] Z. Huang, Y. Mou, X. Xu, D. Zhao, Y. Lai, Y. Xu, C. Chen, P. Li, S. Peng, J. Tian, Y. Zhang,

Novel Derivative of Bardoxolone Methyl Improves Safety for the Treatment of Diabetic Nephropathy, J. Med. Chem. 60 (2017) 8847–8857. https://doi.org/10.1021/acs.jmedchem.7b00971.

[30] E. Bonandi, M.S. Christodoulou, G. Fumagalli, D. Perdicchia, G. Rastelli, D. Passarella, The 1,2,3-triazole ring as a bioisostere in medicinal chemistry, Drug Discov. Today. 22 (2017) 1572–1581. https://doi.org/10.1016/j.drudis.2017.05.014.

[31] G. Wei, W. Luan, S. Wang, S. Cui, F. Li, Y. Liu, Y. Liu, M. Cheng, A library of 1,2,3-triazole-substituted oleanolic acid derivatives as anticancer agents: Design, synthesis, and biological evaluation, Org. Biomol. Chem. 13 (2015) 1507–1514. https://doi.org/10.1039/c4ob01605j.

[32] M. Kanehisa, The KEGG resource for deciphering the genome, Nucleic Acids Res. 32 (2004) 277D – 280. https://doi.org/10.1093/nar/gkh063.

[33] C. von Mering, L.J. Jensen, B. Snel, S.D. Hooper, M. Krupp, M. Foglierini, N. Jouffre, M.A. Huynen, P. Bork, STRING: Known and predicted protein-protein associations, integrated and transferred across organisms, Nucleic Acids Res. 33 (2005) 433–437. https://doi.org/10.1093/nar/gki005.

[34] G. Hoxhaj, B.D. Manning, The PI3K–AKT network at the interface of oncogenic signalling and cancer metabolism, Nat. Rev. Cancer. (2019). https://doi.org/10.1038/s41568-019-0216-7.

[35] J. Luo, B.D. Manning, L.C. Cantley, Targeting the PI3K-Akt pathway in human cancer: Rationale and promise, Cancer Cell. 4 (2003) 257–262. https://doi.org/10.1016/S1535-6108(03)00248-4.

[36] S. Noorolyai, N. Shajari, E. Baghbani, S. Sadreddini, B. Baradaran, The relation between PI3K/AKT signalling pathway and cancer, Gene. 698 (2019) 120–128. https://doi.org/10.1016/j.gene.2019.02.076.

[37] J. Wu, C. Yang, C. Guo, X. Li, N. Yang, L. Zhao, H. Hang, S. Liu, P. Chu, Z. Sun, B. Sun, Y. Lin, J. Peng, G. Han, S. Wang, Z. Tang, SZC015, a synthetic oleanolic acid derivative, induces both apoptosis and autophagy in MCF-7 breast cancer cells, Chem. Biol. Interact. 244 (2016) 94–104. https://doi.org/10.1016/j.cbi.2015.11.013.